ELSEVIER

International Journal of Pressure Vessels and Piping 75 (1998) 75–80

INTERNATIONAL JOURNAL OF
Pressure Vessels and Piping

A new approach to instability testing of shells

Md. Raisuddin Khan[a], M.A. Salam Akanda[b], Md. Wahhaj Uddin[c,*,1]

[a]*BIT, Chittagong, Bangladesh*
[b]*BUET, Dhaka, Bangladesh*
[c]*Tuskegee University, Tuskegee, AL 36088, USA*

Received 18 December 1997; accepted 14 January 1998

Abstract

In this paper, a new experimental technique for the buckling test of shells under external pressure is presented. This technique is simple and determines buckling load very efficiently. It has already been used extensively in the investigation of buckling load of electroformed spherical-tip conical shells under uniform external pressure. In this method, instead of the conventional monitoring of load and linear displacement of points on a shell, load and change in internal volume of the shell are recorded. Internal volumetric change of a shell is found to be a better indicator of its instability compared to the change in displacements of points on its surface. Volumetric change, a function of all the displacements and rotations contributing to the total change in its configuration, is observed to be a highly magnified indicator of shell deformation encompassing the whole shell, primarily the buckling zones and imperfection locations.

Keywords: instability; experimental technique; shells; buckling tests; electroforming; volumetric change

1. Introduction

Experiments on buckling of shells have not yet been standardized. Researchers are continually developing newer experimental techniques, differing from each other, in order to bring about a better correlation between analysis and test. Even when large powerful programs, like STAGS, are employed for analysis, test results still differ considerably from prediction. These differences are partly due to the inaccuracies of inputs like shell geometry, boundary conditions, imperfection in shape, etc., and partly due to variations in buckling behavior of the mathematical model of the shells tested. Experimental results are also found to depend on shell materials and manufacturing techniques.

Experiments on buckling of shells are generally done on their models because conducting experiments on prototypes requires large, costly set-up, and also measuring shell geometry becomes a tedious job. Experimental investigation of shells may be divided into two major steps — the first is the fabrication of model shells and the second is the experimental technique. Isotropic materials are commonly used in fabricating shell models. Shells made of isotropic materials are found to be much more imperfection-sensitive than those of composite materials. So, to achieve better results from isotropic shells, precision manufacturing technology is necessary. Among the different shell fabrication techniques, spin forming, press forming, electroforming, explosive forming and copy milling are in wide use.

Literature on the experimental techniques for buckling tests of shells is limited to a few different methodologies [1–19]. In most cases of shell buckling experiments, very thin shell models are fabricated and, depending upon the opening of the shells, whether open at one end or both, the openings are closed with plates and properly sealed. Through one of the end plates, air is sucked out from the interior of the shell with a vacuum pump so that atmospheric pressure outside the shell acts as an external pressuring medium. The difference between the pressure inside the shell and the atmospheric pressure outside it is considered as the net external pressure. The evacuation process continues until the buckling of the shell starts. Net external pressure at the instant of buckling is considered as the buckling load. To study the load–displacement behavior of a shell, strain gages or displacement probes are placed at the salient points on the shell surface.

In Ref. [14], swedge-stiffened cylinders were tested for buckling under uniform external pressure. The test cylinders were closed at both ends with end-closing plates, keeping atmospheric air inside, and were put into a cylindrical pressure chamber. External pressure was applied to the shells by pumping in water inside the pressure chamber until the

* Corresponding author. Fax: +1 334 727 8177.
[1] On leave from BUET.

0308-0161/98/$19.00
PII: S0308-0161(98)00001-5

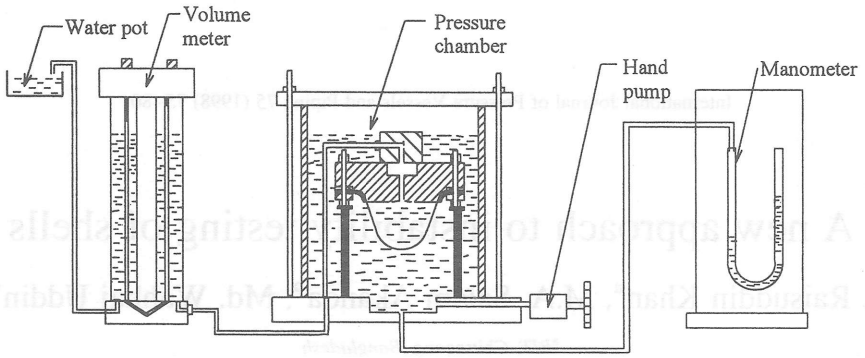

Fig. 1. Schematic diagram of buckling test set-up.

shells buckled with a fall in external pressure. In Ref. [5], instead of using an end-closing plate, a cylinder with two toriconical ends was used. The remaining steps of this experiment are similar to those of Ref. [14].

New and Spring [13] developed a non-destructive experimental technique for determining incipient buckling pressures of thin shells subjected to external pressure. The salient feature of the technique was the filling of the internal volume of the shell with fluid, such as water, to control the magnitude and rate of shell deformation. The incipient buckling pressure was detected by noting the instant at which the difference in internal and external pressure became constant. In Ref. [11] an attempt was made to develop a new non-destructive buckling test technique based on the concept that natural frequency in the buckling mode shape goes to zero when the critical buckling load is reached. By measuring the modal parameters at various load levels below the critical buckling load one should, in principle, be able to predict the buckling load by extrapolating the load frequency interaction curve to zero frequency intercept. But, to date, these non-destructive test methods have received little attention because of the inconveniences associated with the testing procedures.

In test set-ups, where external atmospheric pressure acts as a loading medium, the buckling load must always be less than the atmospheric pressure. This is the major limitation of this technique. Deflection measurement at predetermined locations is another limitation of this method, because, due to imperfections, the shell may not buckle at the locations where deflections are measured. Keeping these disadvantages in mind, in the present work, a new experimental technique is developed. The new method is very simple and capable of finding buckling loads for shells both above and below atmospheric pressure. An electroforming

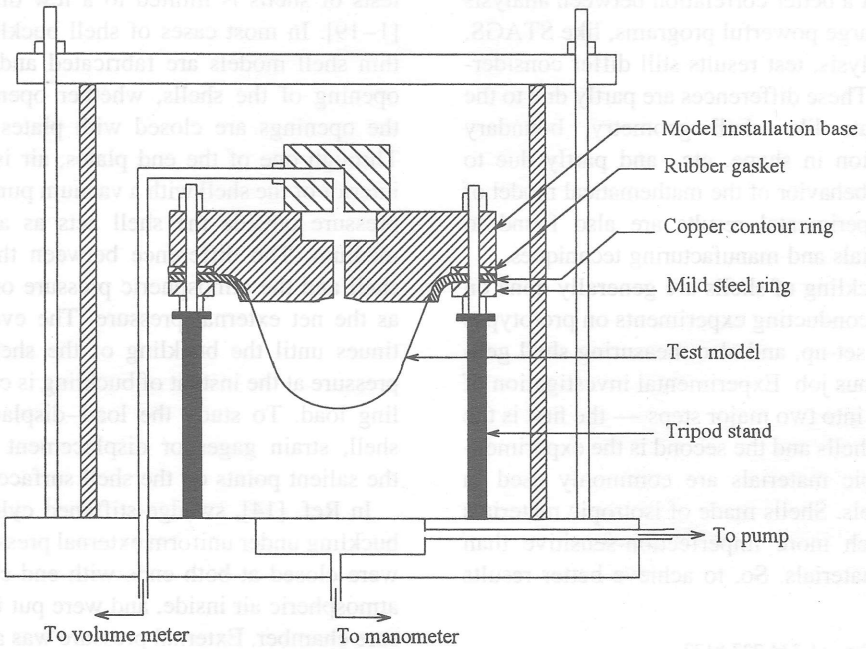

Fig. 2. Schematic diagram of pressure chamber with installed test model.

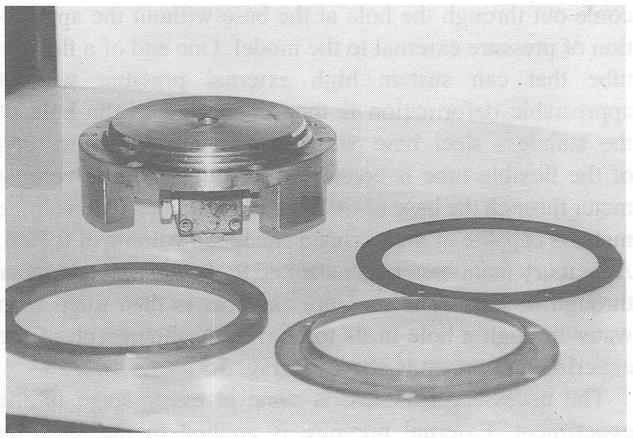

Fig. 3. Test model installation elements.

technique has been employed for the fabrication of shell models for testing. The methodology of the new experimental technique and the experimental set-up are described in the following sections.

2. Present method of experimental investigation

2.1. Experimental methodology

In developing the new experimental technique, it was considered that in the case of thin shells, fabrication imperfection is inevitable and the shells are inherently imperfection-sensitive. Placing of strain gages or displacement probes at the locations of presumed buckling in the conventional experimental techniques may not be able to detect the load displacement behavior of such imperfect shells efficiently. Instead of placing strain gages or displacement probes at the presumed buckling locations, if the internal total volumetric change of the shells is measured, a better picture of instability may evolve, because, volumetric change, an indicator of the total deformation, is a magnified feature of shell displacement encompassing the whole shell including the buckling zone at imperfection locations. It should be noted that monitoring of volumetric deformation does not require precision electronic instrumentation. Considering these facts, the new experimental technique for buckling of shells has been developed based on the measurement of the internal volumetric change of a shell under load.

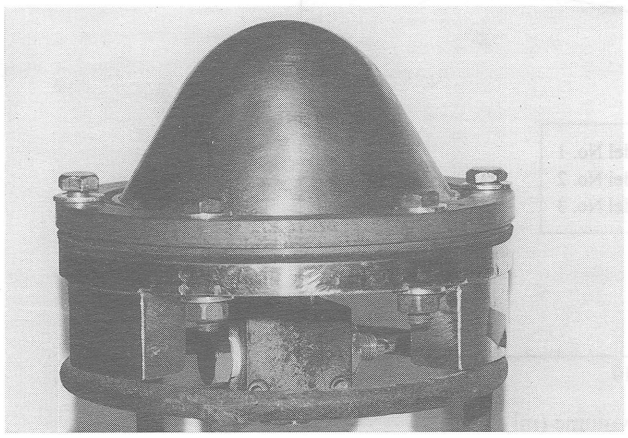

Fig. 4. Test model installed on base.

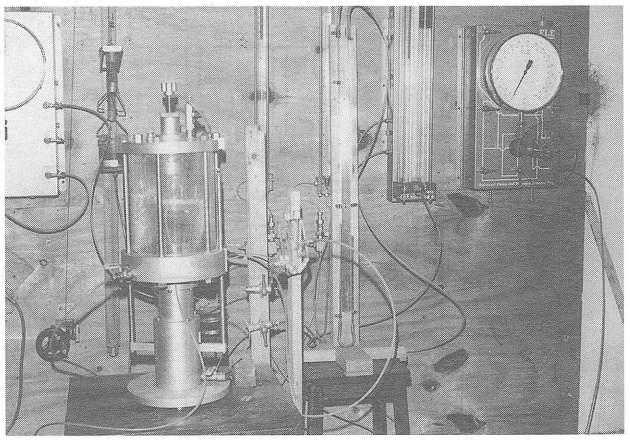

Fig. 5. Experimental set-up.

2.2. Experimental set-up

The set-up consists of a 10 in high, 8 in diameter test chamber, made by ELE, U.K., used as the pressure chamber for the buckling test of the model shells. The wall of the pressure chamber is of transparent Perspex sheet, 0.5 in thick. The limiting pressure of the chamber is 250 psi. The top cover and the bottom platform of the pressure chamber are of metallic plates. The bottom platform can be isolated from the pressure chamber by removing the fastening bolts, so that the experimental models along with attachments can be placed on it. There are a good number of ports on the bottom platform, fitted with glove valves, through which pumps, manometers, pressure gage, volume meter, etc., could be connected. A schematic diagram of the experimental set-up is shown in Fig. 1 and the

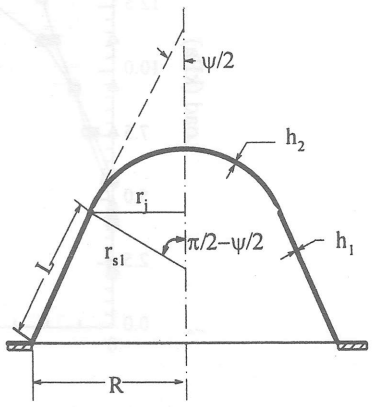

Fig. 6. Geometry of cap–cone composite shell.

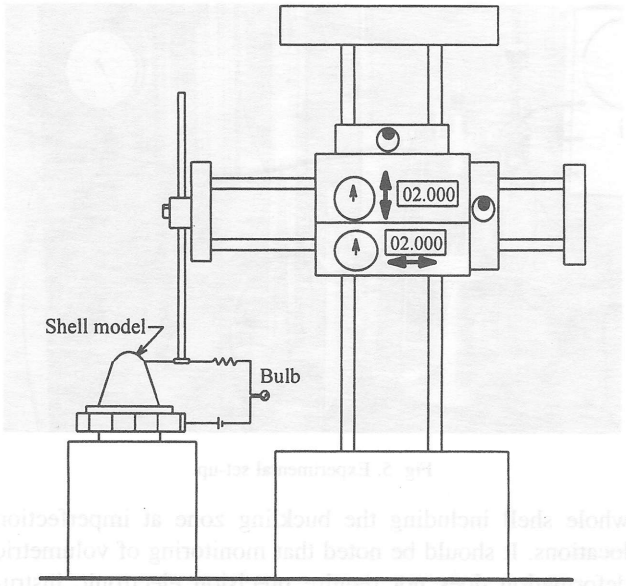

Fig. 7. Schematic diagram of geometry measuring set-up.

details of the test model with base plate assembly along with the pressure chamber are shown in Fig. 2.

2.3. Experimental procedure

To carry out an experiment, the shell model is filled with water and then attached to a stainless steel base-attachment with a metallic ring, a rubber gasket and six 1/4 in fastening bolts. Photographs of the elements of the base-attachment are shown in Fig. 3. The sectional view of the shell base-assembly is shown in Fig. 2. A photograph of the shell base-assembly with the tip of the model up is given in Fig. 4. A tripod is placed inside the pressure chamber to support the base-assembly, with the tip downward and the base-attachment up so that water inside the model cannot come out through the hole at the base without the application of pressure external to the model. One end of a flexible tube that can sustain high external pressure without appreciable deformation is then connected to the hole of the stainless steel base with an adapter. The other end of the flexible tube is connected to a double tube volume meter through the base of the pressure chamber. The volume meter is capable of measuring a change in volume of 0.1 ml. A mercury manometer is connected to the pressure chamber through its base. The pressure chamber is then filled with water through a hole in its top cover. A photograph of the experimental set-up is shown in Fig. 5.

The necessary leak test is done at every stage of the experiment. External pressure is applied to the shell by pumping in water by a hand pump attached to the pressure chamber. The external pressure is applied gradually in steps and, at every step, the pressure is recorded. At any step of external pressure, water coming out from inside the model, which measures the change in its volume, is recorded from the reading of the volume meter. Pressure is increased up to a limit when either the manometer reading remains constant or drops suddenly with a large change in volume. This limiting pressure is considered as the buckling load for the model under test. As the wall of the pressure chamber is transparent, the shape of the shell at every load step is also visually monitored. The limiting pressure is always observed to correspond to a large deformation of the test models.

2.4. Experimental models

A number of conical shells with spherical tip, that is, composite cap–cone shell of varying parameters, were fabricated from copper using an electroforming technique to determine the buckling pressure of shells using the new experimental technique. The cap–cone shells were

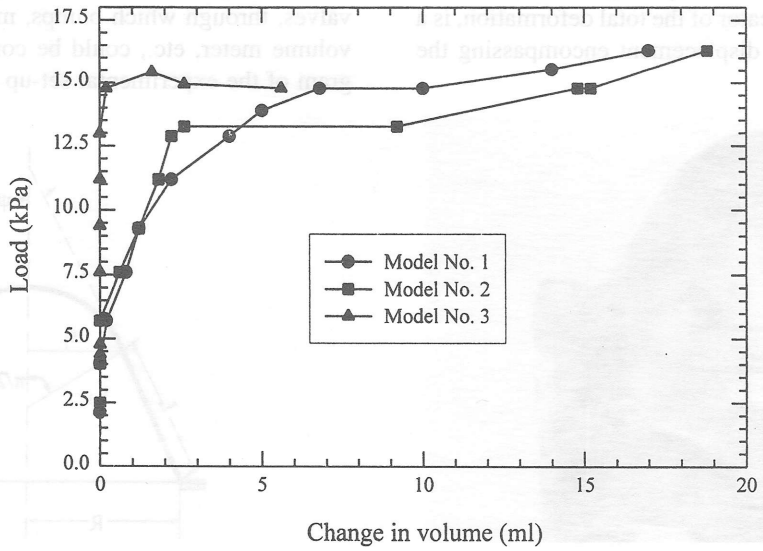

Fig. 8. Trace of the fundamental path of different test models.

Table 1
Geometric data of spherical-tip conical end-closures of shells

Model No.	$\Psi/2°$	L (mm)	R (mm)	r_{s1} (mm)	r (mm)	h_1 (mm)	h_2 (mm)
1	29.886	81.413	58.046	20.16	17.479	0.089	0.127
2	30.174	82.391	57.900	19.08	16.494	0.089	0.101
3	30.029	81.486	57.800	19.66	17.185	0.089	0.114

fabricated maintaining continuity of the slope at the cone–sphere junction. The apex angle of the conical frustum of the cap–cone composite shell was 60°. The geometry of a cap–cone shell is shown in Fig. 6. The geometric parameters of this cap–cone shell are the ratio r/R, the apex angle Ψ of the conical frustum, and the thickness ratio R/h, where r and R are respectively the radii of the cone at the sphere–cone and vessel–cone junctions and h is the thickness of the shell.

2.5. Set-up for imperfection evaluation

Whatever may be the fabrication technique, imperfection is inevitable. In this investigation, imperfections in the geometry of the fabricated shells were measured before conducting the buckling experiment, but the shell thickness was measured after the experiment. Geometric imperfection of each shell was measured after mounting the shell on its base. The base elements, shown in Fig. 3, consist of one stainless steel base, one copper contour ring, one mild steel ring, one rubber 'o' ring (not shown) and six bolts. A sectional view shown in Fig. 2 clearly depicts the shell base-assembly. The stainless base was fabricated by cutting off the die of the electroformed shells, keeping a small conical portion attached to the base. The thick copper contour ring was then electroformed from the base to firmly fix the base of the experimental shells to the base-plate. Finally, the base of the die was machined to a base-attachment to suit the experiment.

The experimental shells and fabricated base-attachments were assembled together and the assembly was placed on a turn-table with the axis of the shell passing through the center of the turn-table. The model base-assembly along with the turn-table was then placed onto a level platform of an x–y–z coordinate measuring instrument, made by Mitutoyo, Japan. The accuracy of the coordinate measuring instrument was $\pm$ 0.01 mm. A fine-wire stylus was attached to the coordinate probe with an electric bulb and a battery in series with the shell to ascertain the contact of the probe with the shell. A schematic diagram of the geometry measuring set-up is shown in Fig. 7. The radii of the shells were then measured against the axial distances of the shells along eight meridians at 45° intervals.

Geometric data of each shell was then processed with a graphical package to find the actual geometry of the shells. Different segmented curves were fitted to each of the meridians of a shell, and the curve set for one meridian corresponding to minimum deviation was selected to represent the geometry of the shell. In case of the cap–cone composite shells, two geometric curves were fitted to the meridians — a straight line to the conical portion of the shell and a circular arc to the spherical cap of the shell, meeting tangentially with the straight line. To determine the thickness of the shells, the shells were cut along three meridians after the experiment, and the thickness along these three meridians was measured with a precision micrometer. The accuracy of the micrometer was $\pm$ 0.001 in. A description of the geometric parameters obtained from processed data, shown in Fig. 6, is given in Table 1.

3. Results and discussion

Experimental results of three models of these shells are presented in column 2 of Table 2. All three models were found to buckle asymmetrically with about six or seven circumferential lobes. The lobes were found to form only in the conical portion of the shells. Load versus volume change curves for these shells, presented in Fig. 8, show that initially, when load is gradually increasing, the change in volume is negligible up to a certain load level and then suddenly becomes almost flat within a few steps of load with a very high rate of change in volume with respect to load. The circumferential lobes were found to form within a few steps of the horizontal portion of the load versus volume curves. After the initiation of the lobes, further attempts at increasing the load made the lobes more prominent with a

Table 2
Experimental and analytical buckling loads of spherical-tip conical end-closures (E for copper is 97.86 GPa)

Model No.	Experimental critical load (P/E)	Asymmetric critical load for cone (P/E)	
		Ends hinged	Ends fixed
1	1.666×10^{-7}(7)	1.94×10^{-7}(8)	1.94×10^{-7}(8)
2	1.577×10^{-7}(7)	1.91×10^{-7}(8)	1.91×10^{-7}(8)
3	1.666×10^{-7}(6)	2.03×10^{-7}(8)	2.04×10^{-7}(8)

Note: numbers in parentheses are the number of circumferential lobes in buckled shells.

large increase in volume for a very small increase in load. At this stage an attempt at load release made the lobes disappear. This indicates that the buckling phenomena of these shells are elastic even in the post-buckling region. To develop a permanent deformation pattern in these shells, the load was increased until the shells collapsed suddenly. In this last phase, the load remained almost unchanged and the deformation pattern got distorted.

Deviation in the geometry of the models, seen in Table 1, is very small from model to model, and the experimental buckling loads for each model are also found to vary slightly. In the third and fourth columns of Table 2, analytical results of instability of the conical portion of these cap–cone models are presented using a computer program based on Reissner's large deflection theory [20,21] for axisymmetric prebuckling analysis, and a linearized version of Sanders' [22] non-linear equations for asymmetric buckling analysis from eigenvalue formulation. The analytical results are found to be about 16 to 21% higher than the experimental results presented here. Deviation in the analytical results of the models is also very small. From the curves of load versus volumetric change, shown in Fig. 8, it is evident that, though the curves maintain a similar trend for all the test models and give very close results, similar models show remarkable deviation of volumetric flow at some load levels just before the occurrence of buckling, which is an indication of imperfections in the models. The imperfections may be either in the geometry or in the boundary attachments. As observed here, the new experimental technique can detect the state of stability of thin shells efficiently and with remarkable precision without using a very precise instrumentation.

4. Conclusions

An experimental technique based on the concept of measuring change of internal volume of a shell under external pressure efficiently determines buckling pressure of shells. Load versus change in internal volume curves can explain the imperfections effect better. Moreover, the technique is very simple and needs no precision instrumentation.

References

[1] Baker EH. Experimental investigation of sandwich cylinders and cones subjected to axial compression. AIAA J., 1968;6(9):1767–1770.

[2] Bushnell D, Galletly GD. Stress and buckling of internally pressurized elastic–plastic torispherical vessel heads: comparison of tests and theory. J. Pressure Vessel Technol., 1977;99:39.

[3] Bushnell D. Nonsymmetric buckling of internally pressurized ellipsoidal and torispherical elastic–plastic pressure vessel heads. J. Pressure Vessel Technol., 1977;99:54.

[4] Bushnell D. Plastic buckling of various shells. J. Pressure Vessel Technol., 1982;104:51.

[5] Galletly GD, Aylward RW, Bushnell D. An experimental and theoretical investigation of elastic and elastic–plastic asymmetric buckling of cylinder–cone combinations subjected to uniform external pressure. Ingenieur-Archiv, 1974;43:345–358.

[6] McCoy JC. An experimental investigation of the general instability of ring stiffened, unpressurized, thin walled cylinders under axial compression. Ph.D. Thesis, California Institute of Technology, 1958.

[7] Penning FA. Experimental buckling modes of clamped shallow shells under concentrated load. ASME J. Appl. Mech., 1966;33(2): 297–304.

[8] Singer J, Bendavid D. Buckling of electroformed conical shells under hydrostatic pressure. AIAA J., 1968;6(12):2332–2338.

[9] Wang LRL. Boundary disturbance and pressure rate on the buckling of spherical caps. AIAA J., 1968;6(11):2192–2193.

[10] Arbocz J. The effect of initial imperfections on shell stability. In: Fung YC, Sechler EE, editors. Thin Shell Structures, Theory, Experiment and Design. Englewood Cliffs, NJ: Prentice-Hall, 1974: 205–245.

[11] Schneider MH Jr, Snell RF, Tracy JJ, Power DR. Buckling and vibration of externally pressurized conical shells with continuous and discontinuous rings. AAIA J., 1991;29(9):1515–1522.

[12] Galletly GD, Blachut J. Elastic buckling of internally pressurized cylinder–bulkhead combinations. Proc. Inst. Eng., 1983;201 (C4): 259–262.

[13] New JC, Spring SM. A nondestructive differential-pressure test for thin shells. J. Appl. Mech., 1953;75:48–52.

[14] Ross CTF, Palmer A. General instability of swedge-stiffened circular cylinders under uniform external pressure. J. Ship Res., 1993;37(1):77–85.

[15] Mamalis AG, Manolakos DE, Viegelahn GL, Vaxevanidis NM, Johnson W. On the inextensional axial collapse of thin PVC conical shells. Int. J. Mech. Sci., 1986;28(5):323–335.

[16] Schroeder FJ, Kusterer ET. An experimental determination of the stability of conical shells. J. Appl. Mech., Trans. ASME 1963; March: 144–146.

[17] Tennyson RC. Buckling modes of circular cylindrical shells under axial compression. AAIA J., 1969;7(8):1481–1487.

[18] Aylward RW, Galletly GD, Moffat DG. Buckling under external pressure of cylinders with toriconical or pierced torispherical ends: a comparison of experiment with theory. J. Mech. Eng. Sci., 1975;17(1):11–18.

[19] Weingarten VI. Elastic stability of thin-walled cylindrical and conical shells under combined external pressure and axial compression. AAIA J., 1965;3(5):913–920.

[20] Reissner E. On the Theory of Thin Elastic Shells, H. Reissner Anniversary Volume. Ann Arbor, MI: JW Edwards, 1949: 231.

[21] Reissner E. On Axisymmetric Deformations of Thin Shells of Revolution. Proc. Symp. Appl. Math., vol. 3. New York: McGraw-Hill; 1950: 27–52.

[22] Sanders JL. Nonlinear theories for thin shells. Q. Appl. Math., 1963;21:21–36.